Loss of *Fgfr1* in chondrocytes inhibits osteoarthritis by promoting autophagic activity in temporomandibular joint

Received for publication, February 6, 2018, and in revised form, April 13, 2018 Published, Papers in Press, April 24, 2018, DOI 10.1074/jbc.RA118.002293

Zuqiang Wang, Junlan Huang, Siru Zhou, Fengtao Luo, Qiaoyan Tan, Xianding Sun, Zhenhong Ni, Hangang Chen, Xiaolan Du[1], Yangli Xie[2], and Lin Chen[3]

From the Department of Rehabilitation Medicine, Center of Bone Metabolism and Repair, State Key Laboratory of Trauma, Burns and Combined Injury, Trauma Center, Research Institute of Surgery, Daping Hospital, Third Military Medical University, Yangzi River Road Number 10, YuZhong District, Chongqing 400042, China

Edited by Xiao-Fan Wang

Temporomandibular joint osteoarthritis (TMJ OA) is a common degenerative disease with few effective disease-modifying treatments in the clinic. Fibroblast growth factor (FGF) signaling is implicated in articular cartilage homeostasis, but the functional roles of FGFR1 in TMJ OA remain largely unknown. In this study, we report that deletion of *Fgfr1* in TMJ chondrocytes delayed TMJ OA progression in the age-associated spontaneous OA model and the abnormal dental occlusion OA model. Immunohistochemical staining revealed that *Fgfr1* deficiency decreased the expressions of MMP13 (matrix metalloproteinase-13), ADAMTS5 (a disintegrin and metalloproteinase with thrombospondin motifs 5), and COL10A1 but increased aggrecan expression level in two TMJ OA models. Furthermore, our data show that inactivation of FGFR1 signaling may promote autophagic activity in TMJ. FGFR1 inhibitor decreased the expressions of *Mmp13*, *Adamts5*, and *Runx2* in IL-1β–stimulated condylar chondrocytes, whereas autophagy inhibitors abrogated the protective effects of the FGFR1 inhibitor. Thus, our study indicates inactivated FGFR1 signaling ameliorates TMJ OA progression partially by promoting autophagic activity. Manipulation of this signaling may be a potential therapeutic approach to modify TMJ OA.

The temporomandibular joint (TMJ)[4] is a load-bearing joint during jaw movement. Normal loading is important for the development and metabolism of TMJ condyle cartilage (1–3). As TMJ bears different levels of mechanical loading in our daily life, temporomandibular disorders is an oral disease with high incidence (4). TMJ osteoarthritis (OA) is one of the most prevalent conditions of temporomandibular disorders, characterized by progressive loss of articular cartilage, chondrocyte hypertrophy, and subchondral bone sclerosis (5, 6). There are few effective therapies to prevent and/or treat TMJ OA. Understanding the cellular and molecular mechanisms of TMJ OA will facilitate the identification of novel therapeutic targets for TMJ OA (7). Currently, multiple signaling pathways, including fibroblast growth factor (FGF), transforming growth factor-β, and Indian hedgehog, have been identified to play critical roles in OA initiation and progression (8, 9). However, the pathogenic mechanism of TMJ OA is still not fully clarified.

FGF family is composed of 22 ligands (FGFs) and 4 tyrosine kinase receptors (FGF receptors (FGFRs)) (10). The FGF-signaling pathway plays important roles in the regulation of skeletal development, which is also involved in the maintenance of articular cartilage (11). In particular, FGFR1 is highly expressed in human chondrocytes in the knee joint. Ellman *et al.* (12) showed that FGF2 plays catabolic roles by activating FGFR1 through its up-regulation of catabolic events, inhibition of proteoglycan synthesis in human articular chondrocytes. Our group previously found that inactivation of FGFR1 signaling can prevent knee joint articular cartilage degeneration in mice (13). In addition, previous studies reported that downstream signaling molecules of FGFR1, such as MEK/ERK, play important roles in the progression of OA (14). All these data suggest that FGFR1 may an play important role in the pathogenesis of TMJ OA. However, the functional roles and potential mechanisms of FGFR1 in TMJ OA remain largely unknown.

Autophagy is an important cellular homeostatic process that provides energy and controls the turnover of damaged organelles and proteins. Impaired autophagic activity is involved in multiple diseases, such as neurodegenerative diseases, infectious diseases, and cardiovascular diseases (15). In chondrocytes, which is characterized by a low rate of cellular turnover, autophagy is essential for maintaining cell survival and function. Previous investigations implicated that autophagy plays an important role in OA progression (16, 17). Autophagy-related proteins, such as Beclin1 and microtubule-associated protein 1A/1B-light chain 3 (LC3), are highly expressed in healthy human and murine articular cartilage, whereas the expressions of these proteins are decreased during OA progression (18). In

This work was supported by Special Funds for Major State Basic Research Program of China (973 Program) Grant 2014CB942904, National Natural Science Foundation of China Grants 81530071 and 81772359, TMMU Doctorate in Military Topics Grant JSKT201608, and Chongqing Foundation & Advanced Research Project Grant cstc2017jcyjAX0148. The authors declare that they have no conflicts of interest with the contents of this article.

This article contains Figs. S1–S4 and Table S1.

[1] To whom correspondence may be addressed. Tel.: 86-023-68757040; Fax: 86-023-68757040; E-mail: dxl_xiaolan@163.com.

[2] To whom correspondence may be addressed. Tel.: 86-023-68757040; Fax: 86-023-68757040; E-mail: xieyangli841015@163.com.

[3] To whom correspondence may be addressed. Tel.: 86-023-68757040; Fax: 86-023-68757040; E-mail: linchen70@163.com.

[4] The abbreviations used are: TMJ, temporomandibular joint; OA, osteoarthritis; FGF, fibroblast growth factor; FGFR, FGF receptor; mTOR, mechanistic target of rapamycin; UAC, unilateral anterior cross-bite; BV/TV, bone volume/total volume; RCS, rat chondrosarcoma; TM, tamoxifen; 3-MA, 3-methyladenine; ECM, extracellular matrix; Tb. Th, trabecular thickness.

addition, Bouderlique *et al.* (19) revealed that genetic deletion of *Atg5* in chondrocytes leads to the development of OA upon aging. Cartilage-specific deletion of mTOR protects articular cartilage from degeneration, and inhibiting mTORC1 with rapamycin also exerts a protective effect on the progression of experimental OA (20, 21). These findings suggest that autophagy in general is a protective mechanism during the development of OA. However, the role of autophagy in TMJ OA, especially its role in the effect of FGFR1 on TMJ OA, has not been fully clarified.

The decreased autophagic activity in *sumf1* (sulfatase-modifying factor 1)-null mice is accompanied by activated FGF signaling in the growth plate, indicating that FGF signaling is involved in the autophagy of chondrocytes (22). In addition, Zhang *et al.* (23) found that FGF signaling activates mTOR resulting in suppressed autophagy through the phosphatidylinositol 3-kinase/AKT signaling pathway. Our group revealed that FGFR3 inhibits the autophagic activity in the pathogenesis of achondroplasia (24). The evidence indicates that FGF signaling may be involved in OA progression by suppressing autophagy activity.

In this study, we found that *Fgfr1* deficiency ameliorates condylar cartilage degeneration in the abnormal dental occlusion OA model and aging-related OA model accompanied by enhanced autophagic activity in TMJ cartilage. Furthermore, our study showed that blockade of autophagy could partially antagonize the protective effect of the FGFR1 inhibitor on condylar chondrocytes treated with IL-1β. Thus, we propose that FGFR1 signaling in chondrocytes negatively regulates TMJ OA progression in part via its inhibition on the autophagic activity.

Results

FGFR1 expression levels are up-regulated in TMJ cartilage with OA

We first evaluated the FGFR1 expression by immunohistochemistry (IHC) in aberrant biomechanical loading of the OA model of TMJ in mice (Fig. S1, *A–D*). In contrast to the weak expression of FGFR1 in condylar chondrocytes of control mice, the expression level of FGFR1 in chondrocytes was gradually increased at the polymorphic layer, the flattened chondrocyte layer, and the hypertrophic layer at 2 and 6 weeks after UAC surgery (Fig. 1, *A–C* and *G*). In addition, we also evaluated the FGFR1 level in condylar cartilage in the age-associated spontaneous OA model. In this model, the expression of FGFR1 was significantly up-regulated at 18 months compared with that at 6 and 12 months (Fig. 1, *D–F* and *H*). These expression profiles strongly implicate a potential role of FGFR1 signaling in the TMJ OA progression.

Fgfr1 deletion delays age-related condylar cartilage degeneration

We next investigated the function of *Fgfr1* in TMJ OA pathogenesis using mice with chondrocyte-specific deletion of FGFR1 (Fig. 1*I*). We determined Cre-mediated recombination efficiency using *Col2a1-CreER^{T2};Rosa26*-tdTomato mice in TMJ. Red fluorescent signals were observed in whole condylar chondrocyte layers except the superficial layer, suggesting high Cre recombination efficiency (85.3%) (Fig. 1, *J–M*). The efficiency of *Fgfr1* deletion in the condylar cartilage, measured by quantitative RT-PCR, reached 61.21% in *Fgfr1$^{f/f}$;Col2a1-CreER^{T2}* (Fgfr1 cKO) mice at 2 months after TM injection (Fig. 1*N*).

We examined the condylar cartilage phenotype of mice with age-associated spontaneous OA. No significantly gross change was observed in the skull and mandible of *Fgfr1* cKO and Cre-negative mice at 6 months (Fig. S2, *A–F*). The sections of TMJ condylar cartilage were stained with Safranin O/fast green, and no significant differences were observed in histology, including cartilage thickness between *Fgfr1* cKO and Cre-negative mice at the age of 6 and 12 months (Fig. 2, *A–D*). At the age of 18 months, Cre-negative mice showed OA-like phenotypes in TMJ cartilage, including spontaneous surface fissures at the superficial layer and polymorphic layer, and loss of Safranin O staining (Fig. 2*E*). In contrast, *Fgfr1* cKO mice showed a comparatively intact structure in TMJ condylar cartilage (Fig. 2*F*). Histological analysis showed that the cartilage thickness was similar between the *Fgfr1* cKO mice and Cre-negative mice at three sampling times (Fig. 2*G*), whereas the percentages of degraded areas in TMJ cartilage were significantly decreased in 18-month-old *Fgfr1* cKO mice (13.71 $\pm$ 3.726%) compared with age-matched Cre-negative mice (58.38 $\pm$ 5.436%) (Fig. 2*H*). Furthermore, using the modified Mankin score system (Table S1), we revealed that TMJ cartilage degeneration was significantly attenuated in 18-month-old *Fgfr1* cKO mice when compared with control littermates (Fig. 2*I*). These results indicate that the development of spontaneous aging-associated TMJ OA is delayed by *Fgfr1* ablation.

Fgfr1 deficiency attenuates condylar cartilage degeneration in UAC-induced TMJ OA model

UAC model was utilized to evaluate the effects of *Fgfr1* deficiency on TMJ OA development induced by abnormal mechanical loading. No significant body weight difference was observed among the four groups at the three sampling times (Fig. S1, *E–G*). 2 weeks after UAC surgery, the intensity of Safranin O staining of TMJ condylar cartilage in the Cre-negative mice appeared to be greatly decreased in most cartilage regions compared with *Fgfr1* cKO mice, but the cartilage thickness showed no significant difference (Fig. 3, *A–H*). At 4 and 6 weeks post-UAC surgery, histological examination showed more severe TMJ cartilage degeneration in Cre-negative mice when compared with respective *Fgfr1* cKO mice (Fig. 3, *I–X*). Then we performed histomorphological analysis to quantify the severity of condylar cartilage damage and found that *Fgfr1* cKO mice showed thicker cartilage with higher cellular density than Cre-negative mice after UAC model (Fig. 3, *Y* and *Z*).

The condylar cartilage degeneration in TMJ OA is now considered to be related to subchondral bone changes (25). Micro-CT evaluation was performed to examine the alterations of subchondral bone after UAC surgery. No significant change was observed at the subchondral bone of *Fgfr1* cKO mice after tamoxifen administration (Fig. 4, *A* and *B*). At 4 weeks post-UAC surgery, the larger cavities were observed in Cre-negative mice compared with *Fgfr1* cKO mice (Fig. 4, *C* and *D*). Furthermore, quantitative data showed that trabecular bone volume (BV/TV) and trabecular thickness (Tb. Th) in subchondral bone from *Fgfr1* cKO were significantly increased compared

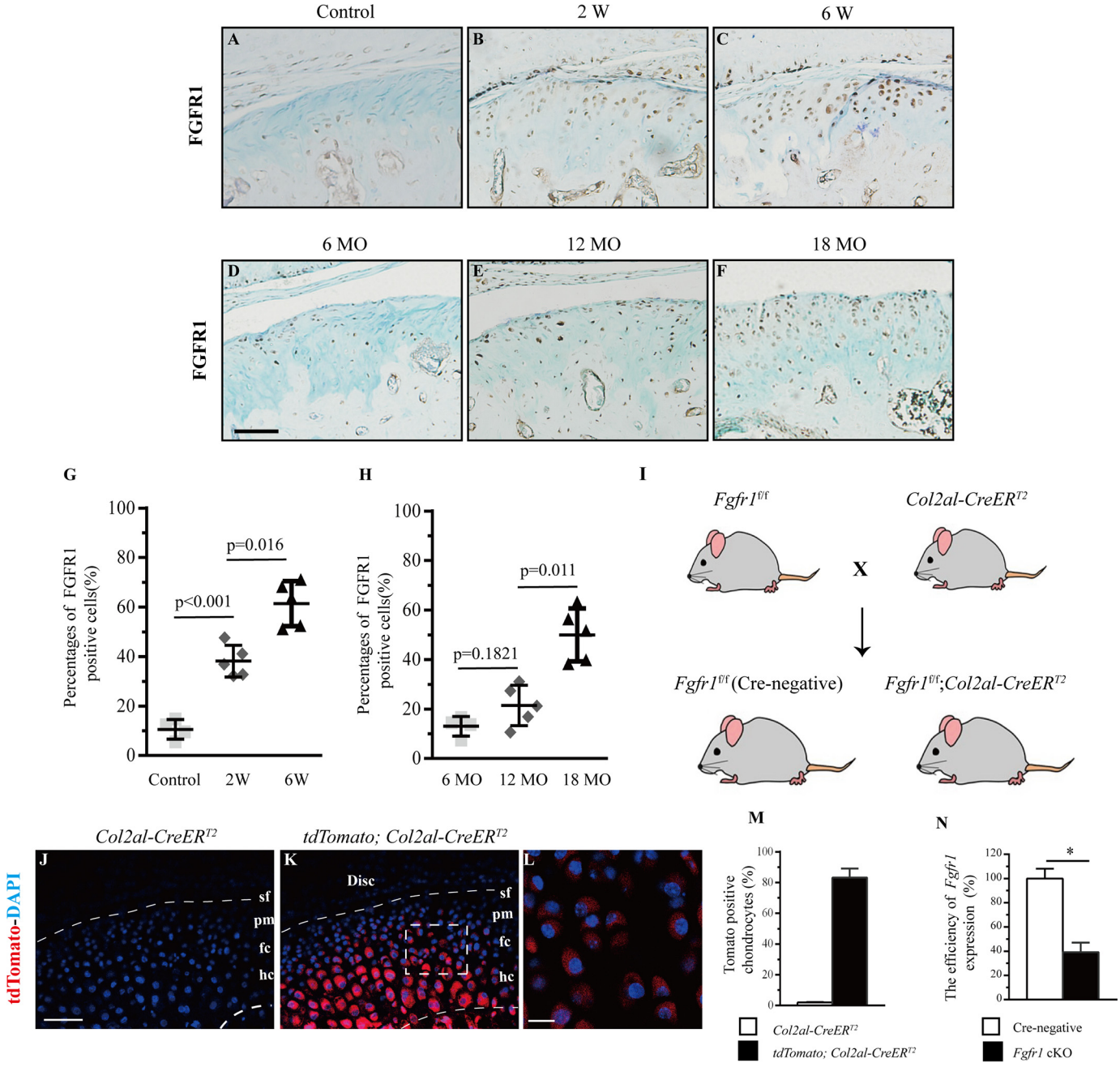

Figure 1. IHC staining for FGFR1 was performed in TMJ condylar cartilage of WT mice (*A*) and nonsurgery mice (*B* and *C*) 2 and 6 weeks (*W*) after UAC surgery. *D–F*, FGFR1 expressions in condylar cartilage of 6-, 12-, and 18-month-old (*MO*) mice. The percentages of FGFR1 immunoreactive positive cells in UAC surgery (*G*) and aging (*H*) TMJ OA models were analyzed ($n = 5–6$ per group). *I*, scheme of experiment: *Fgfr1*$^{f/f}$ mice were crossed with *Col2a1-CreER*^{T2} mice to generate *Fgfr1*$^{f/f}$*;Col2a1-CreER*^{T2} and control mice. *J–M*, representative TMJ sections from *Col2a1-CreER*^{T2}*;Rosa26* tdTomato mice showing the high Cre recombination. *N*, efficiency of *Fgfr1* deletion in TMJ cartilage from *Fgfr1* cKO mice after tamoxifen administration was examined by quantitative-PCR ($n = 3$ per group). *Scale bar*, 50 μm (*A–F*), 100 μm (*J* and *K*), and 200 μm (*L*). Data are expressed as the percent expression relative to controls. Values represent mean (symbols) ± S.D. (*error bar*). *p* values between groups with * are less than 0.05.

with that in Cre-negative control mice after UAC surgery (Fig. 4, *E–G*). These results indicate that deletion of *Fgfr1* delays TMJ OA progression induced by UAC surgery.

Fgfr1 ablation maintains the homeostasis of condylar cartilage

To investigate the underlying mechanism for the attenuated progression of TMJ OA in *Fgfr1* cKO mice, we performed IHC to investigate the pathological changes in two OA models. In the age-associated TMJ OA model, immunostaining data revealed lower expression levels of MMP13, ADAMTS5, and COL10A1 in the condylar cartilage of *Fgfr1* cKO mice compared with that of Cre-negative mice (Fig. 5, *A–T*). Meanwhile, we also examined these catabolic markers in the UAC-induced OA model and found decreased expressions of MMP13, ADAMTS5, and COL10A1 and increased expression of ACAN in *Fgfr1* cKO mice compared with Cre-negative mice at 4 weeks after UAC surgery (Fig. S3, *A–T*). During OA, it is suggested

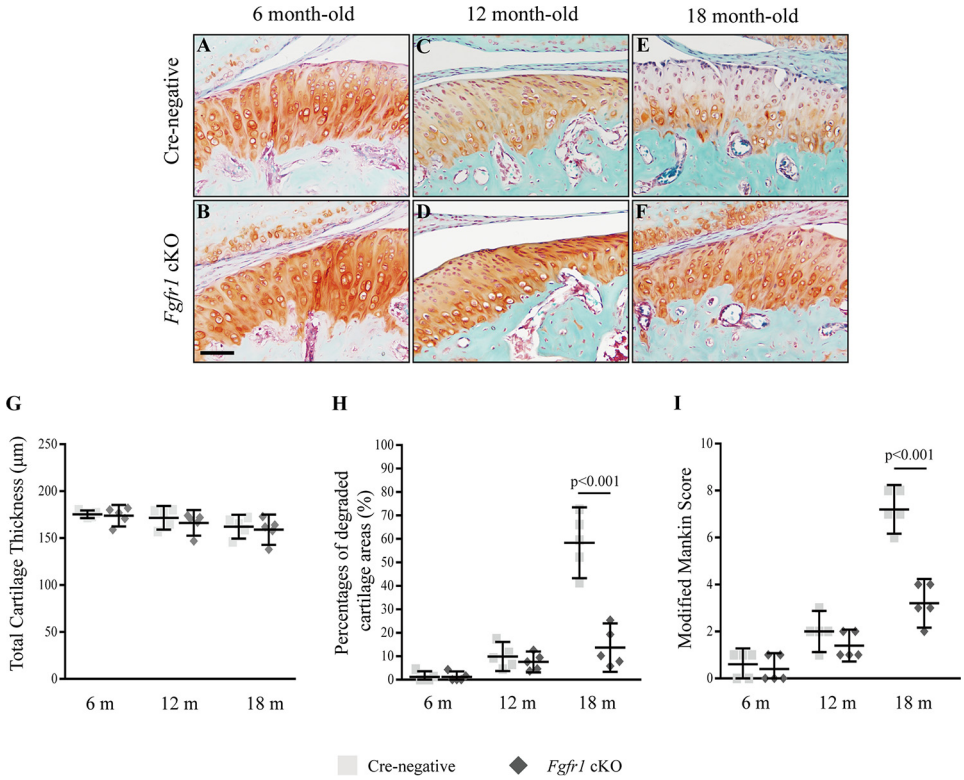

Figure 2. Histological analysis of the condylar cartilage from Cre-negative and *Fgfr1* cKO mice with age-associated spontaneous OA model. *A–F,* representative Safranin O/Fast Green-stained sections in TMJ joints from Cre-negative and *Fgfr1* cKO mice at age of 6, 12, and 18 months (*m*) ($n = 5–6$ per group). *G* and *H,* TMJ condylar cartilage thicknesses and percentages of degraded areas were measured by histomorphometric analysis. *I,* severity of condylar cartilage damage evaluated by a modified Rankin score system. *Scale bar,* 100 μm (*A–F*). Data are expressed as mean (*symbols*) ± S.D. (*error bars*).

that RUNX2 regulates chondrocyte hypertrophy and expressions of ECM-degrading enzymes, and a previous study has shown that activating *Fgfr1* mutation (P250R mutation) could affect the expression of RUNX2. In our two TMJ OA models, immunostaining results showed decreased expressions of phospho-FGFR1 and RUNX2 in *Fgfr1* cKO mice when compared with control littermates (Fig. 6, *A–T*).

Furthermore, we isolated condylar cartilage from TMJ under a stereomicroscope at 4 weeks after the UAC model. RT-PCR results showed that the expressions of *Mmp13*, *Adamts5*, *Col10a1,* and *Runx2* were decreased by 3.4-, 1.62-, 3.03-, and 1.31-fold in *Fgfr1* cKO mice, respectively, compared with Cre-negative mice after UAC surgery (Fig. 6, *U–Y*). These RT-PCR data were consistent with our immunostaining data (Fig. S3, *A–L* and Fig. 6, *E–H*). Collectively, these findings suggest that *Fgfr1* deficiency decreases the catabolic activity in condylar cartilage.

Inactivation of Fgfr1 increases autophagic activity in condylar cartilage

Previous studies implicated that autophagy exerts a protective role in OA progression. To explore the cellular mechanisms underlying the attenuated progression of TMJ OA in *Fgfr1* cKO mice, we examined the effect of FGFR1 signaling on autophagy *in vivo* and *in vitro*. First, we detected the protein level of microtubule-associated protein 1 light chain 3α (MAP1LC3a, hereafter referred to as LC3), a classic marker for autophagosomes membrane, in condylar cartilage by immunofluorescence assay. The results showed that LC3 was expressed in condylar cartilage, and the percentages of cells with LC3 puncta were increased in *Fgfr1* cKO mice compared with that of Cre-negative controls at the age of 2 months (Fig. 7, *A–C*). Then, primary condylar chondrocytes from *Fgfr1* cKO and Cre-negative mice were isolated and treated with 4-hydroxytamoxifen for 3 days. The conversions from the cytosolic protein LC3-I to the lapidated membrane-bound LC3-II, an indicator of autophagic activity, were examined by Western blotting using specific antibodies. Our results revealed that the ratio of LC3-II/LC3-I was increased by 2.5-fold in *Fgfr1* cKO mice when compared with Cre-negative mice (Fig. 7, *D* and *E*). We also determined the protein level of p62/SQSTM1, a known LC3-binding protein. Western blot analysis revealed that p62/SQSTM1 protein levels were reduced by 4-fold in TMJ cartilage of *Fgfr1* cKO mice compared with that of control mice (Fig. 7, *D* and *F*). Furthermore, we employed the rat chondrosarcoma (RCS) cell line to examine the effect of FGFR1 signaling on autophagy. Our results showed that the ratio of LC3-II/LC3-I was significantly decreased in RCS cells with transient transfection of myc-FGFR1 compared with empty vector-transfected cells (Fig. 7, *G* and *H*). By IHC staining, we also found the increased autophagic activity in condylar cartilage of *Fgfr1* cKO mice compared with Cre-negative mice in two TMJ OA models (Fig. 7, *I–R*). These results suggested that inactivation of FGFR1 signaling leads to enhanced autophagic activity in condylar cartilage, which may play an important role in the pathogenesis of TMJ OA.

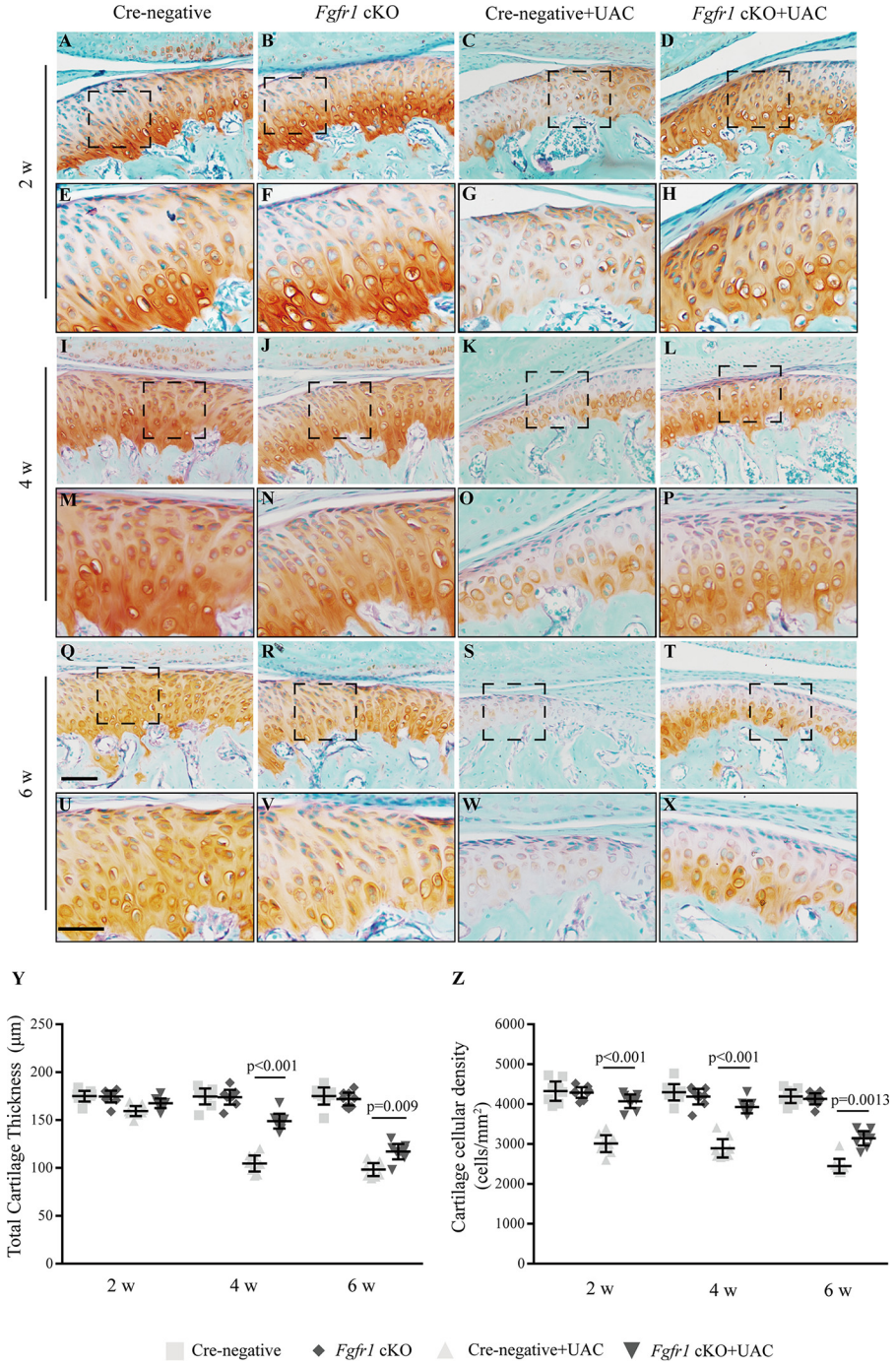

Figure 3. Histology of the TMJ cartilage from Cre-negative and *Fgfr1* cKO mice following UAC surgery. *A–X,* TMJ samples were harvested at 2, 4, and 6 weeks (*w*) post-UAC surgery and analyzed histologically by Safranin O-Fast Green staining. High magnification views of the *boxed areas* are shown ($n = 7–9$ per group). *Y,* thickness of TMJ cartilage was measured by histomorphometric analysis. *Z,* changes of the cellular density in condylar cartilage after UAC surgery. *Scale bar,* 200 μm (*A–D*, *I–L*, and *Q–T*) and 50 μm (*E–H*, *M–P*, and *U–X*). Data are expressed as mean (*symbols*) ± S.D. (*error bars*).

Inhibitors of autophagy suppress the protective effects of G141 in IL-1β–treated condylar chondrocytes

Previously, our group found a non-ATP– dependent FGFR1 inhibitor, G141, and we showed that G141 treatment attenuated the knee joint cartilage degeneration induced by destabilization of the medial meniscus surgery in mice (26). Then we examined whether G141 treatment could inhibit the catabolic events induced by IL-1β in the primary chondrocytes of condylar cartilage. Real-time PCR was used to quantify the expressions of *Mmp13*, *Adamts5, Acan*, *Col10a1*, *Col2a1*, and *Runx2.* Consistent with the results of IHC staining except for *Col10a1*, G141 treatment significantly alleviated the IL-1β–induced catabolic events in condylar chondrocytes (Fig. 8, *A–F*).

HES-1 is an essential molecule of Notch signaling. Loss of *Hes-1* delays osteoarthritis progression via down-regulation of Il-6 and Il1rl1, which are known as pro-inflammatory cytokines in OA (27). Our results showed that G141 treatment decreased IL-1β–mediated up-regulation of *Hes-1* expression in chon-

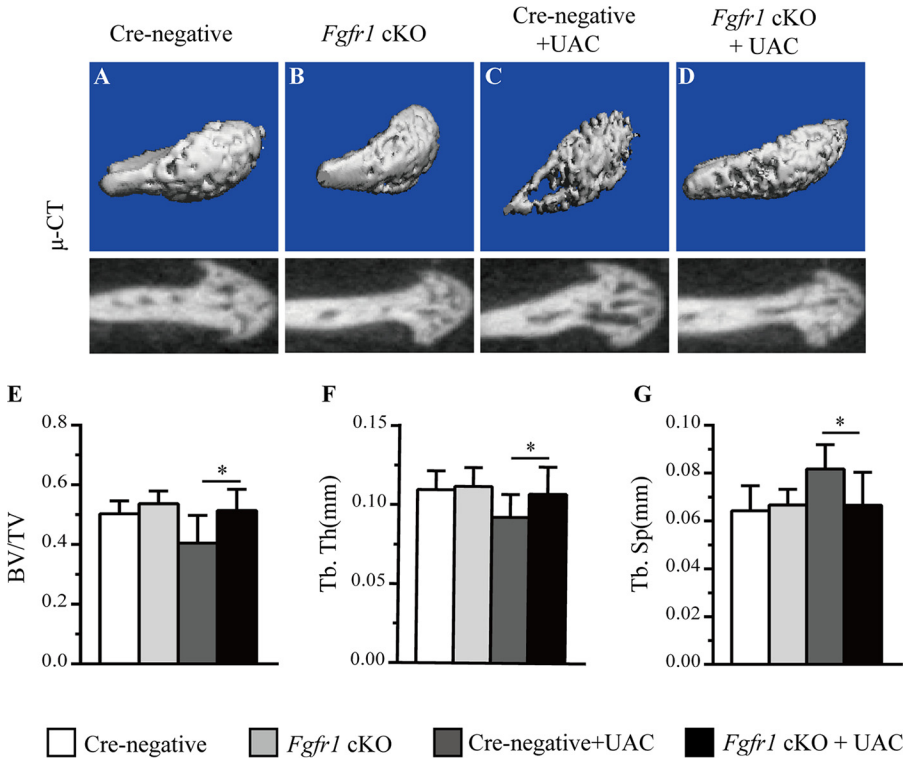

Figure 4. *A–D,* micro-CT 3D reconstructions of subchondral bone in Fgfr1 cKO and Cre-negative mice with or without UAC surgery. *E,* BV/TV. *F,* trabecular thickness (*Tb.Th*), and *G,* trabecular separation (*Tb.Sp*) were measured in the subchondral bone of TMJ condylar cartilage ($n = 4–5$ per group). Values represent mean (*symbols*) ± S.D. (*error bars*). *p* values between groups with * are less than 0.05.

drocytes (Fig. 8*G*). The AP-1 transcription factor consists of either the heterodimer of Jun and Fos proteins or the homodimer of two Jun proteins. AP-1 is known to be involved in the IL-1β activation pathway leading to MMP-13 induction (28). AP-1 is also expressed in articular cartilage (29). This evidence indicates that blocking AP-1–signaling pathways may have chondroprotective effects in cartilage degeneration. Our data showed that the expression of *Ap-1* was significantly decreased in IL-1β–treated chondrocytes with FGFR1 inhibition (Fig. 8*H*). These data suggested that the decreased expressions of *Hes-1* and *Ap-1* may also participate in regulation of inactivated FGFR1 signaling on OA development.

It is suggested that enhanced autophagic activity exerts protective roles during the development of OA, which may be a potential mechanism underlying the attenuated TMJ OA development observed in *Fgfr1* cKO mice. Thus, we examined the effect of two autophagy inhibitors, 3-MA and chloroquine, on the catabolic and anabolic activities in IL-1β–stimulated primary condylar chondrocytes treated with or without G141 treatment. Western blotting results showed the ratio of LC3-II/LC3-I was increased with G141 treatment when compared with autophagy inhibitor 3MA (Fig. 8*I*). Furthermore, compared with that of the untreated group, *Mmp13*, *Adamts5*, and *Runx2* mRNA levels were up-regulated in two groups treated with either 3-MA or chloroquine except for *Col2a1* and *Acan* mRNA levels (Fig. 8, *J–N*). These results suggest that *Fgfr1* deletion attenuates TMJ OA progression partially via promoting autophagy signaling (Fig. 8*O*).

Discussion

TMJ OA is a widespread degenerative disease in adult characterized by progressive loss of proteoglycan and cartilage. So far, there are few effective treatments to prevent and delay the cartilage degeneration in TMJ, resulting from the largely unknown molecular and cellular mechanism. In this study, we first propose that inactivation of FGFR1 signaling at the adult stage attenuates the development of TMJ OA.

Gain-of-function mutation of FGFR1 has been found to cause Pfeiffer syndrome, a kind of craniosynostosis, which is confirmed by using the mouse model carrying gain-of-function mutation of FGFR1 (30). Because ofthe abnormal craniofacial development resulting from gain-of-function mutation in FGFR1 or embryonic lethality of global *Fgfr1* knockout mice, the role of FGFR1 signaling in the homeostasis of adult TMJ condylar cartilage remains largely unknown. To characterize the functions of *Fgfr1* in condylar cartilage homeostasis *in vivo*, we specifically deleted the *Fgfr1* in TMJ cartilage during the adult stage upon two OA models. Histological results showed that *Fgfr1* deletion ameliorates the loss of proteoglycan and structural damage of condylar cartilage in the TMJ, suggesting that *Fgfr1* deficiency has a chondroprotective effect and attenuates the TMJ OA development.

Multiple studies revealed that FGFR1 signaling exerts catabolic effects on chondrocytes to accelerate articular cartilage degeneration in OA progression (31, 32). In this study, we found that the expression levels of *Mmp13*, *Adamts5,* and *Col10a1* were down-regulated in TMJ cartilage of *Fgfr1* cKO mice during the OA process, indicating that inactivation of

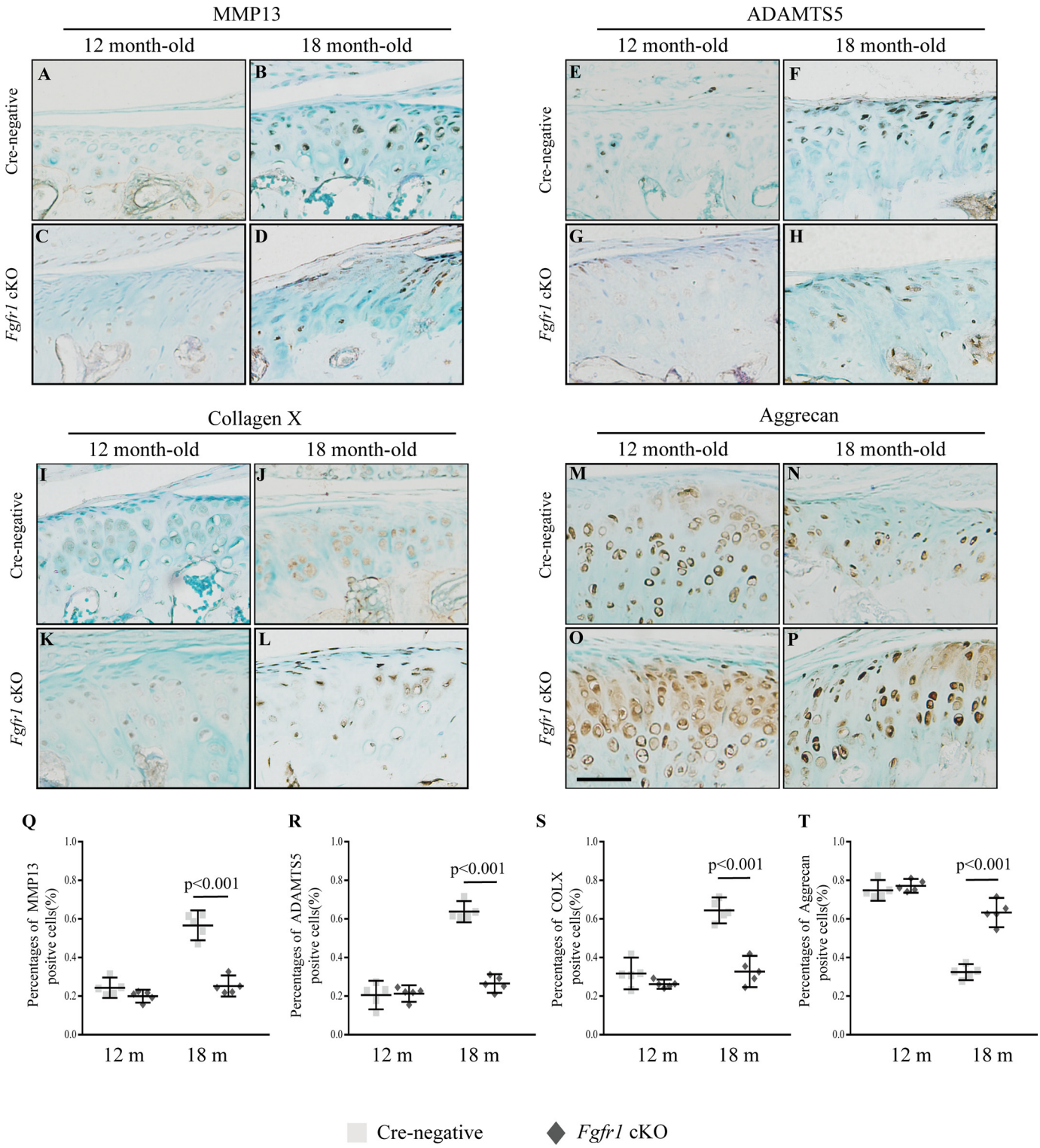

Figure 5. TMJ tissues from 12- to 18-month-old (*m*) mice were analyzed. *A–D,* MMP13; *E–H,* ADAMTS5; *I–L,* COL10A1; and *M–P,* ACAN IHC staining performed in TMJ cartilage of *Fgfr1* cKO mice and Cre-negative ($n = 5$ per group). *Q–T,* percentage of immunoreactive positive cells for MMP13 (*Q*), ADAMTS5 (*R*), COL10A1 (*S*), and ACAN (*T*) were calculated. *Scale bar,* 50 μm (*A–P*). Values represent mean (*symbols*) ± S.D. (*error bars*).

FGFR1 signaling delays condylar cartilage degeneration in the TMJ OA model partially through its inhibition on the catabolic metabolism. The molecular mechanism underlying the catabolic effect of FGFR1 signaling on chondrocytes, however, remains largely unknown. RUNX2 is a well-known transcription factor containing a conserved DNA-binding domain to the *Drosophila* runt gene. RUNX2 plays critical roles in cartilage homeostasis by promoting the expressions of extracellular matrix-degrading enzymes and chondrocyte hypertrophy, resulting in accelerated OA development (33–35). Zhou *et al.* (30) showed that FGFR1 signaling positively regulates intramembranous bone formation through its up-

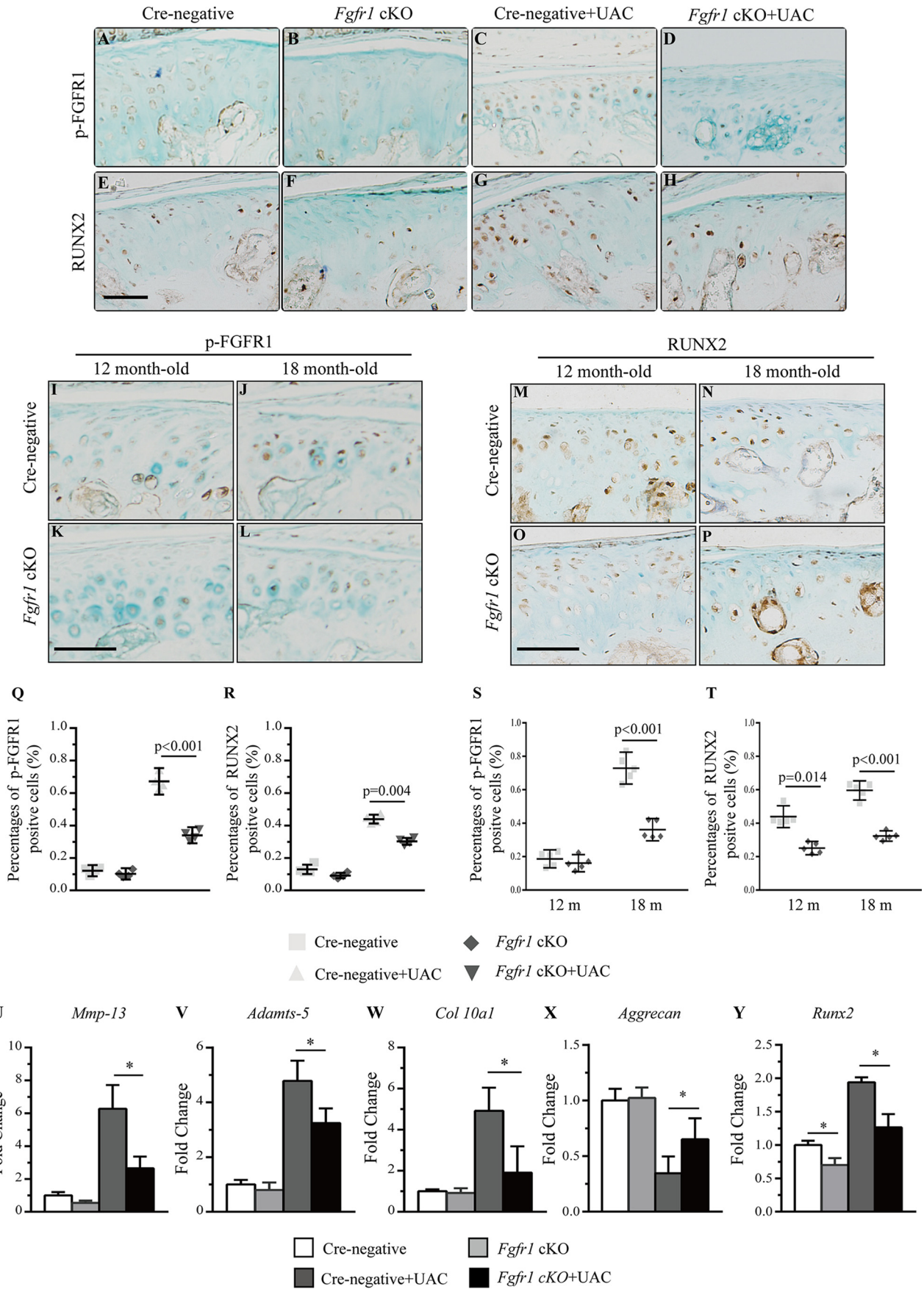
Cre-negative
Fgfr1 cKO
Cre-negative+UAC
Fgfr1 cKO+UAC
p-FGFR1
RUNX2
A
B
C
D
E
F
G
H
p-FGFR1
12 month-old
18 month-old
RUNX2
12 month-old
18 month-old
Cre-negative
Fgfr1 cKO
I
J
K
L
M
N
O
P
Q
R
S
T
Percentages of p-FGFR1 positive cells (%)
Percentages of RUNX2 positive cells (%)
p<0.001
p=0.004
p<0.001
p=0.014
p<0.001
12 m
18 m
Cre-negative
Fgfr1 cKO
Cre-negative+UAC
Fgfr1 cKO+UAC
U
Mmp-13
V
Adamts-5
W
Col 10a1
X
Aggrecan
Y
Runx2
Fold Change
*
Cre-negative
Fgfr1 cKO
Cre-negative+UAC
Fgfr1 cKO+UAC

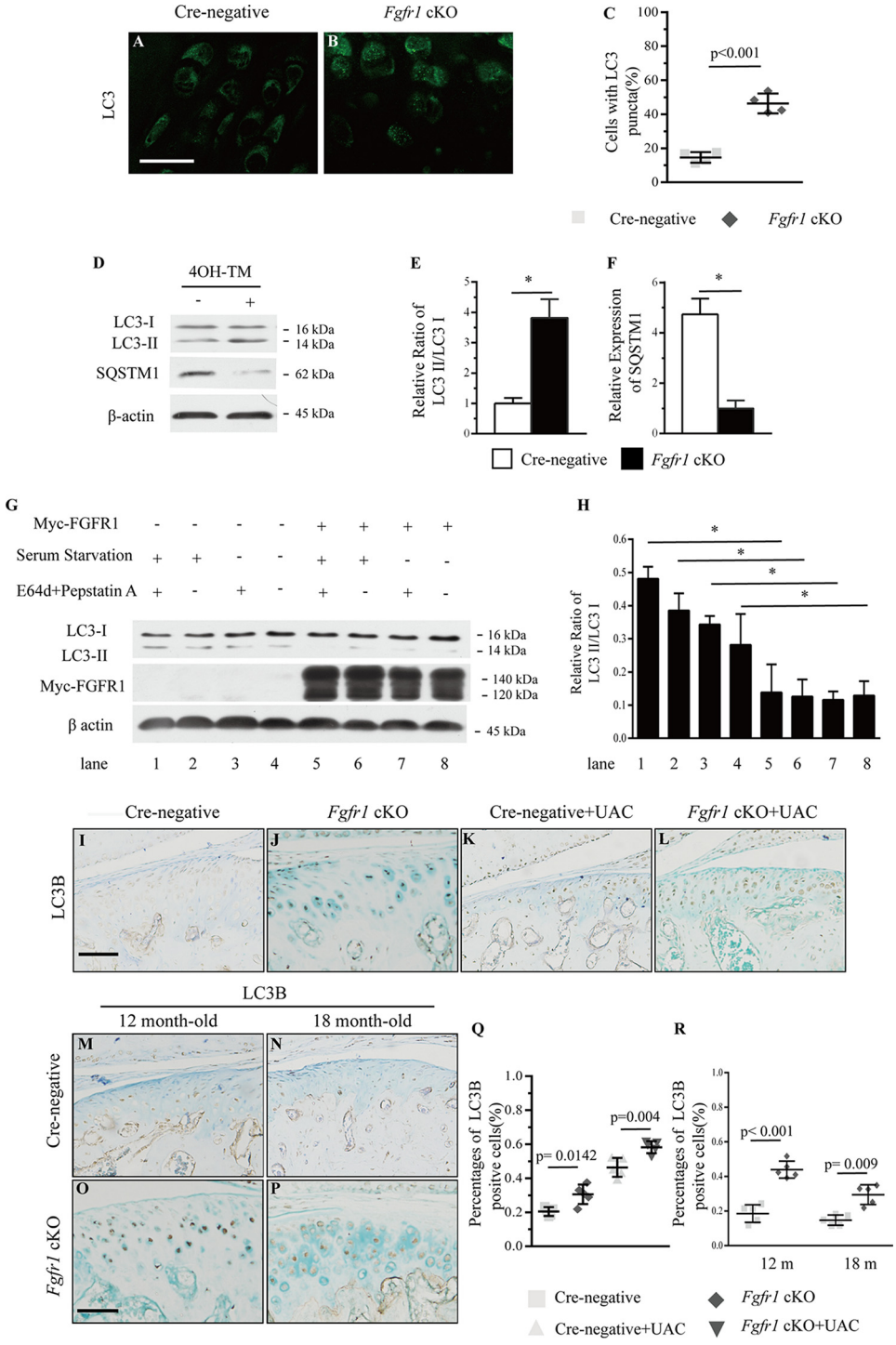

Figure 7. *A* and *B*, LC3 punctate signals were analyzed by immunofluorescence assay from TMJ cartilage of *Fgfr1* cKO and Cre-negative mice at age 6 months. *C*, percentage of cells with LC3 puncta was quantified ($n = 4$ per group). *D*, Western blot analysis of the ratio of LC3-II/LC3-I and SQSTM1 expression in the primary condylar chondrocytes from *Fgfr1* cKO mice. TM-untreated group were used as controls. The signal intensities, LC3-II/-I (*E*) and SQSTM1 (*F*), were quantified using software ImageJ (version 1.47) ($n = 5–6$ per group). *G*, overexpression of myc-FGFR1 in response to serum starvation for 4 h in the presence or absence of E64d and pepstatin A in RCS cells. *H*, signal intensity was analyzed ($n = 3$ per group). The TMJ cartilages were immunohistochemically stained for LC3 in two TMJ OA models ($n = 4–5$ per group). *I–P*, the ratios of immunoreactive LC3B positive cells. *Q* and *R*, LC3-positive cells were quantified. *Scale bar*, 50 μm (*I–P*). Values represent mean (*symbols*) ± S.D. (*error bars*). *p* values between groups with * are less than 0.05. *m*, month.

Figure 6. *A–P*, immunohistochemical detection of phospho-FGFR1 and RUNX2 expression performed in TMJ OA models induced by either surgery or aging ($n = 5–6$ per group). *Q–T*, percentages of phospho-FGFR1 and RUNX2 immunoreactive positive cells. *Q* and *S*, phospho-FGFR1; *R* and *T*, RUNX2-positive cells were quantified. *U–Y*, real-time PCR analysis of *Mmp13*, *Adamts5*, *Col10a1*, *Acan*, and *Runx2* expression in condylar cartilage explants isolated from TMJ of *Fgfr1* cKO and Cre-negative mice 4 weeks after UAC surgery ($n = 4–6$ per group). *Scale bar*, 50 μm (*A–P*). Values represent mean (*symbols*) ± S.D. (*error bars*). *p* values between groups with * are less than 0.05. *m*, month.

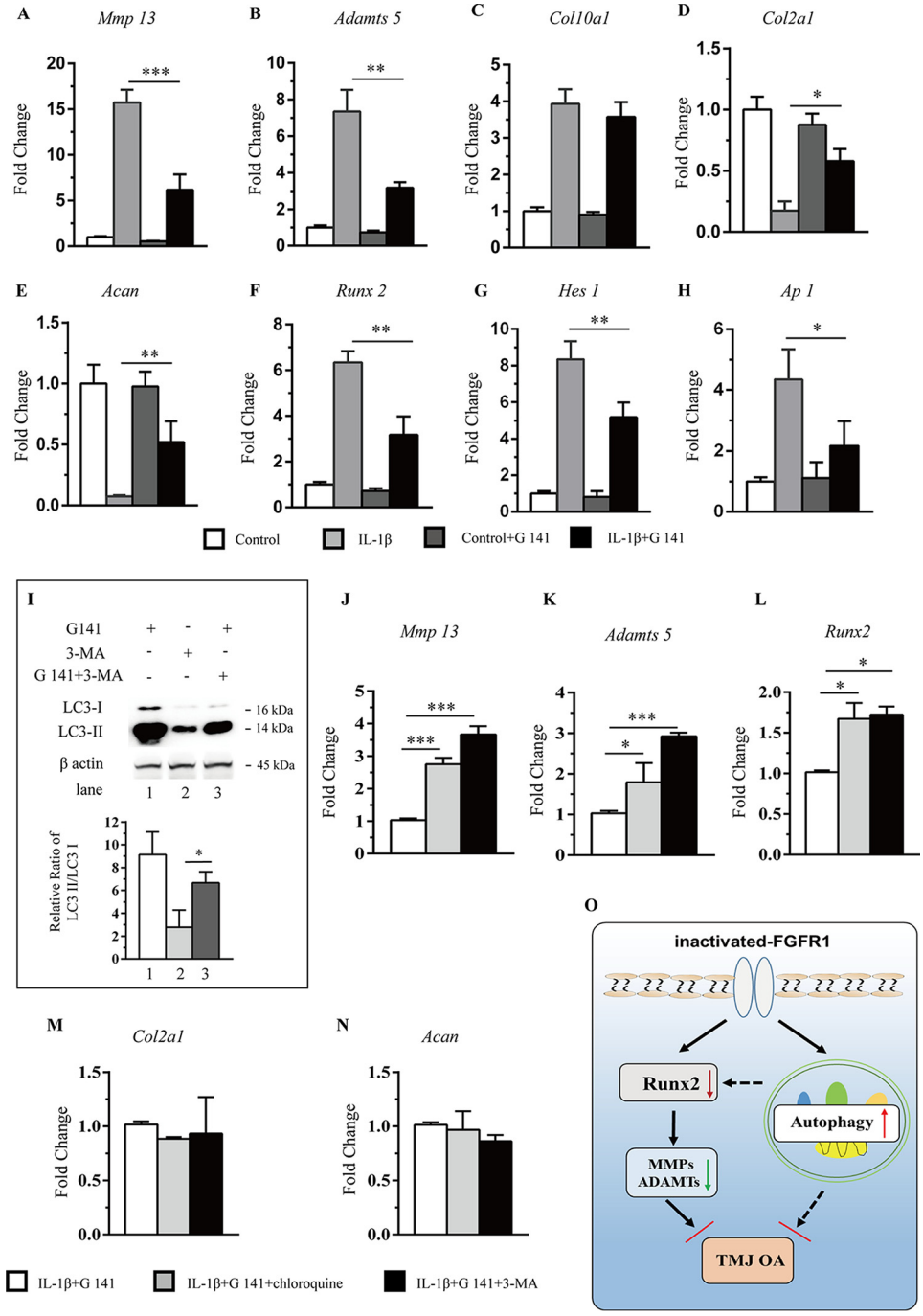

Figure 8. *A–H,* primary condylar chondrocytes were treated with G141 (10 μM) for 1 h, followed by treatment of IL-1β (10 ng/ml) for 24 h. Total RNA was isolated, and mRNAs levels of *Mmp13*, *Adamts5*, *Col10a1*, *Runx2*, *Col2a1*, *Acan*, *Hes-1*, and *Ap-1* were detected by RT-PCR ($n = 3$ per group). *4OH-TM*, 4-hydroxytamoxifen. *I,* Western blot analysis of the ratio of LC3-II/LC3-I expression in chondrocytes. *J–N,* quantitative PCR analysis of gene expressions in condylar chondrocytes treated with of either one of two autophagy inhibitors, 3-MA (10 mM) and chloroquine (50 mM), in G141-treated and IL-1β-stimulated condition ($n = 3$ per group). *O,* schematic diagram of the mechanisms underlying the role of FGFR1 signaling in the maintenance of condylar cartilage in adults TMJ. Values represent mean (*symbols*) ± S.D. (*error bars*). *p* values between groups with * are less than 0.05.

regulation of *Runx2* expression. *Fgfr1* with P250R mutation increases the expression of *Runx2 in vivo* (30). The evidence suggests that FGFR1 may regulate RUNX2 expression in TMJ OA progression. In this study, we found that *Fgfr1* deletion decreased RUNX2 expression both *in vivo* and *in vitro*, suggesting that *Fgfr1* deletion protects TMJ cartilage from degeneration in part through its inhibition on RUNX2 expression.

Recently, autophagy has been considered to play important roles in the cartilage maintenance and progression of OA (36). Several studies revealed that dysregulated autophagy may be implicated in OA. Previously, Zhang *et al.* (37) observed the autophagy in chondrocytes during the early stage of TMJ OA. In this study, we found that FGFR1 signaling inhibits autophagic activity in condylar cartilage both *in vivo* and *in vitro*, indicating that down-regulation of FGFR1 signaling

attenuates TMJ OA development partially via promoting autophagic activity. However, the detailed mechanisms for the regulation of autophagy by FGFR1 signaling during the process of TMJ OA remain to be further determined.

To further confirm the role of autophagy in the protective effects of FGFR1 deficiency on TMJ OA progression, we investigated whether the protective effect of G141, a novel FGFR1 inhibitor, on the IL-1β–stimulated catabolic events in condylar chondrocytes is related to the up-regulated autophagic activity. Our results showed that treatment by either one of two autophagy inhibitors could abrogate the decreases in *Mmp13*, *Adamts5*, and *Runx2* expressions resulting from G141 treatment in IL-1β–treated condylar chondrocytes. Unexpectedly, no remarkable changes in *Col2a1* and *Acan* expressions were observed following treatment of autophagy inhibitors when compared with the control group, indicating that the anabolic effects of FGFR1 deficiency on TMJ cartilage may be independent on autophagy. Cinque *et al.* (38) suggested that regulation of autophagy, mainly mediated through FGFR4, may be co-regulated with anabolic events during bone development. Interestingly, FGFR1 and FGFR3 are highly expressed in human articular chondrocytes (39). Ellman *et al.* (12) showed that FGFR3 is involved in the synthesis of ECM components, and our laboratory previously revealed that deletion of *Fgfr1* increases the expression of FGFR3 in knee joint chondrocytes (13, 23). We also found the increased expression of FGFR3 in TMJ cartilage of *Fgfr1* cKO mice compared with Cre-negative mice after UAC surgery (Fig. S4, *A–E*). Whether FGFR3 is involved in the anabolic effects of FGFR1 deficiency on TMJ OA requires further investigation. This question could be studied by using genetic modulation approaches such as condylar chondrocyte-specific double *Fgfr1* and *Fgfr3* knockout mice, which is now ongoing.

In conclusion, we found that *Fgfr1* deficiency in condylar chondrocytes attenuates TMJ OA development induced by surgery and aging, partially via promoting the autophagic activity in TMJ. Our findings indicate that FGFR1 plays an injurious role during TMJ OA progression, which helps to understand the mechanism of TMJ OA and facilitate the searching for effective therapies for TMJ OA.

Experimental procedures

Animals

Fgfr1$^{f/f}$ mice (*Fgfr1* floxed) and *Col2a1-CreER*^{T2} mice were genotyped as described previously (13). *Fgfr1*$^{f/f}$ mice were crossed with *Fgfr1*$^{f/f}$;*Col2a1-CreER*^{T2} mice to obtain *Fgfr1*$^{f/f}$;*Col2a1-CreER*^{T2} (*Fgfr1* cKO) and *Fgfr1*$^{f/f}$ (Cre-negative, Control) mice. Both *Col2a1-CreER*^{T2} and *Fgfr1*$^{f/f}$ mice were in the C57BL/6J background. Tamoxifen (TM; Sigma) was administered by intraperitoneal (i.p.) injection in male *Fgfr1* cKO mice and male Cre-negative littermates at the age of 8 weeks (1 mg/10 g body weight, daily for 5 days). Cre-mediated recombination efficiency was measured by breeding *Col2a1-CreER*^{T2} mice with *Rosa26*-tdTomato reporter mice. TM was administered to 2-month-old mice, and the mice were sacrificed at 4 months to determine recombination efficiency. All mice were maintained in the animal facility (specific pathogen-free level) of the Daping Hospital (Chongqing, China). All experiments were performed according to protocols approved by the Laboratory Animal Welfare and Ethics Committee of Third Military Medical University (Chongqing, China).

Mouse model of TMJ OA

The UAC surgery was performed on the left maxillary and mandibular incisors of 8-week-old male mice after 5 days of TM injections according to the methods described previously (3, 40). For the UAC OA model, mice of each genotype randomly divided into two groups (with or without UAC) were sacrificed at 2, 4, and 6 weeks postoperatively (n = 7–9 per group). For the spontaneous OA model, *Fgfr1* cKO and Cre-negative mice were administered tamoxifen injections for 5 day at 2 months, and TMJ samples were harvested at 6, 12, and 18 months (n = 5–6 per group).

Histological assessment

The TMJ specimen was fixed in 4% paraformaldehyde, decalcified in 15% EDTA/PBS, and embedded in paraffin. Serial sagittal sections were obtained across the TMJ tissue by collecting 5-μm sections at 40-μm intervals. The sections of TMJ cartilage were stained by Safranin O/Fast Green. Microscopic scoring of mouse TMJ condylar cartilage degeneration was performed utilizing a modified Mankin score system according to a previous study (41). All investigators were blinded to allocation in experiments and outcome assessments. Scoring was carried out by three independent investigators. For histomorphometric analysis, the cartilage thickness and cartilage cellular density were quantified by Image-Pro Plus 5.1 (Leeds Precision Instruments, Minneapolis, MN).

Immunohistochemistry

Immunohistochemistry was performed using SP-9000 Histostain-Plus kits (ZSGB-BIO, Beijing, China). Briefly, decalcified TMJ tissues were deparaffinized with xylene, and endogenous peroxidase activity was quenched by 3% H_2O_2 for 15 min, followed by antigen retrieval with trypsinase for 15 min. The tissues sections were then treated with antigen retrieval using 0.1% trypsin and blocked with goat serum for 30 min. Sections were incubated overnight at 4 °C with antibodies against the following proteins: FGFR1 (1:100 dilution; Santa Cruz Biotechnology, Dallas, TX); p-FGFR1 (1:100 dilution; Santa Cruz Biotechnology); COL10A1 (1:400 dilution; Abcam, Cambridge, MA); MMP13 (1:300 dilution; Proteintech, Chicago); ADAMTS5 (1:200 dilution; Abcam); aggrecan (1:200 dilution; Millipore, Billerica, MA); RUNX2 (1:200 dilution; Santa Cruz Biotechnology); and LC3B (1:200 dilution; Sigma). After rinsing with PBS, horseradish peroxidase (HRP)-conjugated secondary antibody was applied and stained with a DAB kit. The number of positive cells in the condylar cartilage section was quantified by Image-Pro Plus 5.1.

Immunofluorescence staining and confocal laser scanning

Slides were washed with PBS and incubated with blocking solution (1% BSA in PBS) for 30 min and then exposed to anti-LC3B antibody (1:200 dilution; Sigma) at 4 °C overnight. After washing three times with blocking solution, slides were incubated to secondary antibodies. The TMJ chondrocytes were

recorded using a confocal microscope (Zeiss LSM880, Germany). The percentage of cells with LC3 puncta was quantified according to a previous study. Cre-mediated recombination efficiency in *Col2a1-CreER^{T2}*;Rosa26-tdTomato mice was determined using Zeiss LSM880 confocal microscope.

Isolation of condylar cartilage and culture of primary chondrocytes

Mice were sacrificed at 4 weeks after UAC surgery, and the condylar cartilage was exposed by blunt dissection as described previously (42). The condylar cartilage was isolated from the subchondral bone under a stereomicroscope and pulverized for RNA extraction.

The chondrocytes of condylar cartilage were isolated from 8-week-old mice after 5 days of TM injections. Dissected tissues with cartilage were first digested with 0.25% trypsinase (Gibco/Life Technologies, Inc.) at 37 °C for 15 min. After removal of muscles, ligaments, and bone tissue, TMJ cartilage was digested with 0.1% collagenase II (Gibco/Life Technologies, Inc.) overnight at 37 °C in a CO_2 incubator. Isolated TMJ chondrocytes were seeded onto 12-well plates at 10^6 cells per well and cultured in DMEM/F-12 containing 10% FBS for 3 days. The condylar chondrocytes were incubated with G141 (10 μM), IL-1β (10 ng/ml) (Peprotech), 3-MA (10 mM) (M9281, Sigma), and chloroquine (50 mM) (C6628, Sigma).

Cell line culture and treatment

RCS cells were cultured in DMEM/F-12 (1:1), supplemented with 5% FBS. Transient transfection (myc-FGFR1) was performed with VigoFect (T001, Vigorous) in accordance with the manufacturer's protocols. For serum starvation, RCS cells were cultured in serum-free medium for 4 h in the presence or absence of E64d (1 ng/ml) (E8640, Sigma) and pepstatin A (1 ng/ml) (77170, Sigma).

Real-time PCR

Total RNA was extracted from TMJ cartilage tissues and chondrocytes using TRIzol reagent (Invitrogen/Life Technologies, Inc.). Total RNA was reverse-transcribed to cDNA using PrimerScript RT reagent kit (Takara Biotechnology, Otsu, Japan). Relative gene expression was measured with MxPro software provided by the manufacturer (Stratagene, Santa Clara, CA). All samples were measured in triplicate and normalized to internal control cyclophilin A.

X-ray and micro-CT analysis

X-ray images of TMJ tissue were obtained by using an MX-20 Cabinet X-ray system (Faxitron X-Ray, Tucson, AZ). The TMJ tissues were scanned with a Scanco Viva CT 40 instrument (Scanco Medical, Brüttisellen, Switzerland) and analyzed for subchondral bone density according to our previous studies (43, 44). Serial 10.5-μm 2D and 3D images were obtained at 70 kV and 113 mA. Constant thresholds (210) were used to gray scale images to distinguish bone from soft tissue.

Western blotting

The proteins of TMJ chondrocytes were extracted by RIPA lysis buffer containing protease inhibitors (Roche Applied Science). Equal protein samples were resolved by 10 or 12% SDS-polyacrylamide gel and transferred onto a polyvinylidene difluoride membrane (Millipore, Billerica, MA). After being blocked with 8% nonfat milk in TBS/Tween buffer, the membrane was probed with primary and secondary antibodies, followed by detection of the chemiluminescent signal (Pierce, 34080).

Statistical analysis

The data were expressed as the mean ± S.D. Differences between two groups were evaluated by unpaired Student's *t* test. One-way analysis of variance was used for comparisons of multiple groups followed by Bonferroni test in this study. Data were analyzed using GraphPad Prism version 6.01 software (GraphPad Inc., La Jolla, CA) and SPSS 19.0 program (IBM, New York). $p < 0.05$ is considered statistically significant.

Author contributions—Z. W., J. H., F. L., Q. T., Z. N., H. C., X. D., Y. X., and L. C. conceptualization; Z. W. data curation; Z. W., F. L., Z. N., H. C., X. D., and Y. X. validation; Z. W., J. H., S. Z., Q. T., X. S., Z. N., H. C., X. D., Y. X., and L. C. investigation; Z. W., F. L., Q. T., Z. N., H. C., X. D., Y. X., and L. C. writing-original draft; Z. W., Q. T., H. C., X. D., Y. X., and L. C. project administration; Z. W., J. H., F. L., Q. T., Z. N., H. C., X. D., Y. X., and L. C. writing-review and editing; J. H., F. L., X. S., Z. N., H. C., X. D., Y. X., and L. C. formal analysis; J. H., S. Z., X. S., Z. N., and X. D. supervision; J. H., F. L., Q. T., X. S., Z. N., H. C., X. D., Y. X., and L. C. methodology; S. Z., F. L., X. S., Z. N., H. C., X. D., and Y. X. resources; S. Z., X. S., Z. N., and X. D. software; Q. T., H. C., X. D., Y. X., and L. C. funding acquisition.

Acknowledgments—We thank our colleagues for valuable suggestions and discussion. We also thank Meng Xu and Dali Zhang for technical assistance.

References

1. Milam, S. B. (2005) Pathogenesis of degenerative temporomandibular joint arthritides. *Odontology* **93,** 7–15 CrossRef Medline
2. Horio, T., and Kawamura, Y. (1989) Effects of texture of food on chewing patterns in the human subject. *J. Oral Rehabil.* **16,** 177–183 CrossRef Medline
3. Liu, Y. D., Liao, L. F., Zhang, H. Y., Lu, L., Jiao, K., Zhang, M., Zhang, J., He, J. J., Wu, Y. P., Chen, D., and Wang, M. Q. (2014) Reducing dietary loading decreases mouse temporomandibular joint degradation induced by anterior crossbite prosthesis. *Osteoarthritis Cartilage* **22,** 302–312 CrossRef Medline
4. Tanaka, E., Detamore, M. S., and Mercuri, L. G. (2008) Degenerative disorders of the temporomandibular joint: etiology, diagnosis, and treatment. *J. Dent. Res.* **87,** 296–307 CrossRef Medline
5. Zarb, G. A., and Carlsson, G. E. (1999) Temporomandibular disorders: osteoarthritis. *J. Orofac. Pain* **13,** 295–306 Medline
6. Luder, H. U., Leblond, C. P., and von der Mark, K. (1988) Cellular stages in cartilage formation as revealed by morphometry, radioautography and type II collagen immunostaining of the mandibular condyle from weanling rats. *Am. J. Anat.* **182,** 197–214 CrossRef Medline
7. Wang, X. D., Zhang, J. N., Gan, Y. H., and Zhou, Y. H. (2015) Current understanding of pathogenesis and treatment of TMJ osteoarthritis. *J. Dental Res.* **94,** 666–673 CrossRef
8. Tang, J., Su, N., Zhou, S., Xie, Y., Huang, J., Wen, X., Wang, Z., Wang, Q., Xu, W., Du, X., Chen, H., and Chen, L. (2016) Fibroblast growth factor receptor 3 inhibits osteoarthritis progression in knee joints of adult mice. *Arthritis Rheumatol.* **68,** 2432–2443 CrossRef Medline
9. Zhen, G., Wen, C., Jia, X., Li, Y., Crane, J. L., Mears, S. C., Askin, F. B., Frassica, F. J., Chang, W., Yao, J., Carrino, J. A., Cosgarea, A., Artemov, D.,

Chen, Q., Zhao, Z., *et al.* (2013) Inhibition of TGF-β signaling in mesenchymal stem cells of subchondral bone attenuates osteoarthritis. *Nat. Med.* **19,** 704–712 CrossRef Medline
10. Ornitz, D. M., and Itoh, N. (2015) The fibroblast growth factor signaling pathway. *Wiley Interdiscip. Rev Dev. Biol.* **4,** 215–266 CrossRef Medline
11. Su, N., Jin, M., and Chen, L. (2014) Role of FGF/FGFR signaling in skeletal development and homeostasis: learning from mouse models. *Bone Res.* **2,** 14003 CrossRef Medline
12. Ellman, M. B., An, H. S., Muddasani, P., and Im, H. J. (2008) Biological impact of the fibroblast growth factor family on articular cartilage and intervertebral disc homeostasis. *Gene* **420,** 82–89 CrossRef Medline
13. Weng, T., Yi, L., Huang, J., Luo, F., Wen, X., Du, X., Chen, Q., Deng, C., Chen, D., and Chen, L. (2012) Genetic inhibition of FGFR1 in cartilage attenuates articular cartilage degeneration in adult mice. *Arthritis Rheum.* **64,** 3982–3992 CrossRef Medline
14. Martin, G., Bogdanowicz, P., Domagala, F., Ficheux, H., and Pujol, J. P. (2003) Rhein inhibits interleukin-1 β-induced activation of MEK/ERK pathway and DNA binding of NF-κB and AP-1 in chondrocytes cultured in hypoxia: a potential mechanism for its disease-modifying effect in osteoarthritis. *Inflammation* **27,** 233–246 CrossRef Medline
15. Choi, A. M., Ryter, S. W., and Levine, B. (2013) Autophagy in human health and disease. *N. Engl. J. Med.* **368,** 651–662 CrossRef Medline
16. Lotz, M. K., and Caramés, B. (2011) Autophagy and cartilage homeostasis mechanisms in joint health, aging and OA. *Nat. Rev. Rheumatol.* **7,** 579–587 CrossRef Medline
17. Carames, B., Olmer, M., Kiosses, W. B., and Lotz, M. K. (2015) The relationship of autophagy defects to cartilage damage during joint aging in a mouse model. *Arthritis Rheum.* **67,** 1568–1576 CrossRef
18. Sasaki, H., Takayama, K., Matsushita, T., Ishida, K., Kubo, S., Matsumoto, T., Fujita, N., Oka, S., Kurosaka, M., and Kuroda, R. (2012) Autophagy modulates osteoarthritis-related gene expression in human chondrocytes. *Arthritis Rheum.* **64,** 1920–1928 CrossRef Medline
19. Bouderlique, T., Vuppalapati, K. K., Newton, P. T., Li, L., Barenius, B., and Chagin, A. S. (2016) Targeted deletion of Atg5 in chondrocytes promotes age-related osteoarthritis. *Ann. Rheum. Dis.* **75,** 627–631 CrossRef Medline
20. Zhang, Y., Vasheghani, F., Li, Y. H., Blati, M., Simeone, K., Fahmi, H., Lussier, B., Roughley, P., Lagares, D., Pelletier, J. P., Martel-Pelletier, J., and Kapoor, M. (2015) Cartilage-specific deletion of mTOR upregulates autophagy and protects mice from osteoarthritis. *Ann. Rheum. Dis.* **74,** 1432–1440 CrossRef Medline
21. Caramés, B., Hasegawa, A., Taniguchi, N., Miyaki, S., Blanco, F. J., and Lotz, M. (2012) Autophagy activation by rapamycin reduces severity of experimental osteoarthritis. *Ann. Rheum. Dis.* **71,** 575–581 CrossRef Medline
22. Settembre, C., Arteaga-Solis, E., McKee, M. D., de Pablo, R., Al Awqati, Q., Ballabio, A., and Karsenty, G. (2008) Proteoglycan desulfation determines the efficiency of chondrocyte autophagy and the extent of FGF signaling during endochondral ossification. *Genes Dev.* **22,** 2645–2650 CrossRef Medline
23. Zhang, J., Liu, J., Huang, Y., Chang, J. Y., Liu, L., McKeehan, W. L., Martin, J. F., and Wang, F. (2012) FRS2α-mediated FGF signals suppress premature differentiation of cardiac stem cells through regulating autophagy activity. *Circ. Res.* **110,** e29–e39 CrossRef Medline
24. Wang, X., Qi, H., Wang, Q., Zhu, Y., Wang, X., Jin, M., Tan, Q., Huang, Q., Xu, W., Li, X., Kuang, L., Tang, Y., Du, X., Chen, D., and Chen, L. (2015) FGFR3/fibroblast growth factor receptor 3 inhibits autophagy through decreasing the ATG12-ATG5 conjugate, leading to the delay of cartilage development in achondroplasia. *Autophagy* **11,** 1998–2013 CrossRef Medline
25. Chen, J., Sorensen, K. P., Gupta, T., Kilts, T., Young, M., and Wadhwa, S. (2009) Altered functional loading causes differential effects in the subchondral bone and condylar cartilage in the temporomandibular joint from young mice. *Osteoarthritis Cartilage* **17,** 354–361 CrossRef Medline
26. Xu, W., Xie, Y., Wang, Q., Wang, X., Luo, F., Zhou, S., Wang, Z., Huang, J., Tan, Q., Jin, M., Qi, H., Tang, J., Chen, L., Du, X., Zhao, C., *et al.* (2016) A novel fibroblast growth factor receptor 1 inhibitor protects against cartilage degradation in a murine model of osteoarthritis. *Sci. Rep.* **6,** 24042 CrossRef Medline
27. Sugita, S., Hosaka, Y., Okada, K., Mori, D., Yano, F., Kobayashi, H., Taniguchi, Y., Mori, Y., Okuma, T., Chang, S. H., Kawata, M., Taketomi, S., Chikuda, H., Akiyama, H., Kageyama, R., *et al.* (2015) Transcription factor Hes1 modulates osteoarthritis development in cooperation with calcium/calmodulin-dependent protein kinase 2. *Proc. Natl. Acad. Sci. U.S.A.* **112,** 3080–3085 CrossRef Medline
28. Boileau, C., Pelletier, J. P., Tardif, G., Fahmi, H., Laufer, S., Lavigne, M., and Martel-Pelletier, J. (2005) The regulation of human MMP-13 by licofelone, an inhibitor of cyclo-oxygenases and 5-lipoxygenase, in human osteoarthritic chondrocytes is mediated by the inhibition of the p38 MAP kinase signalling pathway. *Ann. Rheum. Dis.* **64,** 891–898 CrossRef Medline
29. Karreth, F., Hoebertz, A., Scheuch, H., Eferl, R., and Wagner, E. F. (2004) The AP1 transcription factor Fra2 is required for efficient cartilage development. *Development* **131,** 5717–5725 CrossRef Medline
30. Zhou, Y. X., Xu, X., Chen, L., Li, C., Brodie, S. G., and Deng, C. X. (2000) A Pro250Arg substitution in mouse Fgfr1 causes increased expression of Cbfa1 and premature fusion of calvarial sutures. *Hum. Mol. Genet.* **9,** 2001–2008 CrossRef Medline
31. Yan, D., Chen, D., and Im, H. J. (2012) Fibroblast growth factor-2 promotes catabolism via FGFR1-Ras-Raf-MEK1/2-ERK1/2 axis that coordinates with the PKCδ pathway in human articular chondrocytes. *J. Cell. Biochem.* **113,** 2856–2865 CrossRef Medline
32. Li, X., Ellman, M. B., Kroin, J. S., Chen, D., Yan, D., Mikecz, K., Ranjan, K. C., Xiao, G., Stein, G. S., Kim, S. G., Cole, B., van Wijnen, A. J., and Im, H. J. (2012) Species-specific biological effects of FGF-2 in articular cartilage: implication for distinct roles within the FGF receptor family. *J. Cell. Biochem.* **113,** 2532–2542 CrossRef Medline
33. Shen, J., Li, J., Wang, B., Jin, H., Wang, M., Zhang, Y., Yang, Y., Im, H. J., O'Keefe, R., and Chen, D. (2013) Deletion of the transforming growth factor β receptor type II gene in articular chondrocytes leads to a progressive osteoarthritis-like phenotype in mice. *Arthritis Rheum.* **65,** 3107–3119 CrossRef Medline
34. Wang, X., Manner, P. A., Horner, A., Shum, L., Tuan, R. S., and Nuckolls, G. H. (2004) Regulation of MMP-13 expression by RUNX2 and FGF2 in osteoarthritic cartilage. *Osteoarthritis Cartilage* **12,** 963–973 CrossRef Medline
35. Kamekura, S., Kawasaki, Y., Hoshi, K., Shimoaka, T., Chikuda, H., Maruyama, Z., Komori, T., Sato, S., Takeda, S., Karsenty, G., Nakamura, K., Chung, U. I., and Kawaguchi, H. (2006) Contribution of runt-related transcription factor 2 to the pathogenesis of osteoarthritis in mice after induction of knee joint instability. *Arthritis Rheum.* **54,** 2462–2470 CrossRef Medline
36. Caramés, B., Taniguchi, N., Otsuki, S., Blanco, F. J., and Lotz, M. (2010) Autophagy is a protective mechanism in normal cartilage, and its aging-related loss is linked with cell death and osteoarthritis. *Arthritis Rheum.* **62,** 791–801 CrossRef Medline
37. Zhang, M., Zhang, J., Lu, L., Qiu, Z. Y., Zhang, X., Yu, S. B., Wu, Y. P., and Wang, M. Q. (2013) Enhancement of chondrocyte autophagy is an early response in the degenerative cartilage of the temporomandibular joint to biomechanical dental stimulation. *Apoptosis* **18,** 423–434 CrossRef Medline
38. Cinque, L., Forrester, A., Bartolomeo, R., Svelto, M., Venditti, R., Montefusco, S., Polishchuk, E., Nusco, E., Rossi, A., Medina, D. L., Polishchuk, R., De Matteis, M. A., and Settembre, C. (2015) FGF signalling regulates bone growth through autophagy. *Nature* **528,** 272–275 CrossRef Medline
39. Yan, D., Chen, D., Cool, S. M., van Wijnen, A. J., Mikecz, K., Murphy, G., and Im, H. J. (2011) Fibroblast growth factor receptor 1 is principally responsible for fibroblast growth factor 2-induced catabolic activities in human articular chondrocytes. *Arthritis Res. Ther.* **13,** R130 CrossRef Medline

40. Lu, L., Huang, J., Zhang, X., Zhang, J., Zhang, M., Jing, L., Yu, S., and Wang, M. (2014) Changes of temporomandibular joint and semaphorin 4D/Plexin-B1 expression in a mouse model of incisor malocclusion. *J. Oral Facial Pain Headache* **28,** 68–79 CrossRef Medline
41. Zhou, S., Xie, Y., Li, W., Huang, J., Wang, Z., Tang, J., Xu, W., Sun, X., Tan, Q., Huang, S., Luo, F., Xu, M., Wang, J., Wu, T., Chen, L., Chen, H., Su, N., Du, X., Shen, Y., and Chen, L. (2016) Conditional deletion of Fgfr3 in chondrocytes leads to osteoarthritis-like defects in temporomandibular joint of adult mice. *Sci. Rep.* **6,** 24039 CrossRef Medline
42. Schminke, B., Muhammad, H., Bode, C., Sadowski, B., Gerter, R., Gersdorff, N., Bürgers, R., Monsonego-Ornan, E., Rosen, V., and Miosge, N. (2014) A discoidin domain receptor 1 knock-out mouse as a novel model for osteoarthritis of the temporomandibular joint. *Cell. Mol. Life Sci.* **71,** 1081–1096 CrossRef Medline
43. de Bont, L. G., van der Kuijl, B., Stegenga, B., Vencken, L. M., and Boering, G. (1993) Computed tomography in differential diagnosis of temporomandibular joint disorders. *Int. J. Oral Maxillofac. Surg.* **22,** 200–209 CrossRef Medline
44. Yang, T., Zhang, J., Cao, Y., Zhang, M., Jing, L., Jiao, K., Yu, S., Chang, W., Chen, D., and Wang, M. (2015) Wnt5a/Ror2 mediates temporomandibular joint subchondral bone remodeling. *J. Dental Res.* **94,** 803–812 CrossRef